nature climate change

LETTERS

PUBLISHED ONLINE: 11 APRIL 2016 | DOI: 10.1038/NCLIMATE2991

Anthropogenic forcing dominates global mean sea-level rise since 1970

Aimée B. A. Slangen[1,2*], John A. Church[1], Cecile Agosta[3], Xavier Fettweis[3], Ben Marzeion[4] and Kristin Richter[5]

Sea-level change is an important consequence of anthropogenic climate change, as higher sea levels increase the frequency of sea-level extremes and the impact of coastal flooding and erosion on the coastal environment, infrastructure and coastal communities[1,2]. Although individual attribution studies have been done for ocean thermal expansion[3,4] and glacier mass loss[5], two of the largest contributors to twentieth-century sea-level rise, this has not been done for the other contributors or total global mean sea-level change (GMSLC). Here, we evaluate the influence of greenhouse gases (GHGs), anthropogenic aerosols, natural radiative forcings and internal climate variability on sea-level contributions of ocean thermal expansion, glaciers, ice-sheet surface mass balance and total GMSLC. For each contribution, dedicated models are forced with results from the Coupled Model Intercomparison Project Phase 5 (CMIP5) climate model archive[6]. The sum of all included contributions explains 74 ± 22% (±2σ) of the observed GMSLC over the period 1900–2005. The natural radiative forcing makes essentially zero contribution over the twentieth century (2 ± 15% over the period 1900–2005), but combined with the response to past climatic variations explains 67 ± 23% of the observed rise before 1950 and only 9 ± 18% after 1970 (38 ± 12% over the period 1900–2005). In contrast, the anthropogenic forcing (primarily a balance between a positive sea-level contribution from GHGs and a partially offsetting component from anthropogenic aerosols) explains only 15 ± 55% of the observations before 1950, but increases to become the dominant contribution to sea-level rise after 1970 (69 ± 31%), reaching 72 ± 39% in 2000 (37 ± 38% over the period 1900–2005).

Although the major contributions to twentieth-century GMSLC are known and there has been significant progress in closing the sea-level budget within uncertainties[2,7], knowledge of how the contributions and the total GMSLC have responded to external climate forcings from natural and anthropogenic sources and past climatic changes is incomplete. For ocean thermal expansion (TE), the anthropogenic forcing is responsible for around 85% of the 1970–2005 change[3,4]. However, only 25 ± 35% of the 1851–2010 glacier mass loss is attributable to anthropogenic causes, rising to 69 ± 24% for 1991–2010[5]. A study analysing tide-gauge data alone concluded there was an anthropogenic contribution of at least 45% in the twentieth century[8].

Here we go beyond previous work[3–5,8] and determine the underlying drivers of twentieth-century GMSLC. We use output from CMIP5 climate model experiments[6] driven by historical, anthropogenic, natural, GHG and anthropogenic aerosol radiative forcings. These are used to compute TE, drive a glacier model[9] and compute ice-sheet surface mass balance (SMB)[10], resulting in a consistent model data set for 1900–2005 (Methods, Supplementary Table 1). The pre-industrial CMIP5 control runs are used to estimate internal climate variability.

Under CMIP5 control run forcing, most contributions show little variability, and no significant trend on a centennial timescale (Fig. 1a). However, if the glacier model is initiated to its 1850 state and then forced with control run variability, there is a contribution of 30 ± 13 mm for 1900–2005 (cyan) as a result of the continued retreat of glaciers to higher altitudes after the Little Ice Age (LIA relaxation)[5,11], as glaciers typically take decades to centuries to establish a new equilibrium after climate changes.

Under natural-only forcing, which includes the solar cycle and volcanic eruptions, TE variability is larger (Fig. 1b), but shows no significant long-term trend. The majority of the glacier contribution is due to LIA relaxation (compare blue to dashed cyan line) and shows little discernible response to volcanic eruptions, as glaciers respond more indirectly and on a longer timescale than upper-ocean TE. The glacier LIA contribution explains most of the total change (black), whereas TE (red) dictates the variability.

In the GHG-only experiment (Fig. 1c), glaciers and TE each account for about 50% of the modelled GMSLC. The Greenland SMB contribution is small and the Antarctic SMB has a slightly larger negative contribution. TE reacts directly to the increasing GHG concentrations, particularly from the 1960s onwards, whereas the glacier contribution is initially due to the LIA relaxation, with a growing response to increasing GHG forcing. In contrast, the negative radiative forcing in the anthropogenic aerosol-only experiment (Fig. 1d) results in a fall in TE (−48 ± 23 mm) and Greenland SMB (−12 ± 2 mm). Antarctic SMB and glaciers contribute to sea-level rise, the latter due to the LIA relaxation. Without LIA, the glacier contribution would show a sea-level fall (cyan).

Combining all anthropogenic forcings (Fig. 1e) leads to a substantial sea-level rise, albeit less than in the GHG-only experiment, owing to the counteracting effect of aerosols. The anthropogenic total equals the GHG-only plus the aerosol-only totals minus the LIA relaxation term (which is counted twice if the two experiments are added together). The ratio of TE and glacier contributions is similar in the anthropogenic-only and historical experiments (Fig. 1f), although the addition of natural forcing in the historical experiment introduces naturally forced variability, which is absent in the anthropogenic-only experiment.

[1]CSIRO Oceans & Atmosphere, Hobart, Tasmania 7000, Australia. [2]Institute for Marine and Atmospheric Research Utrecht (IMAU), Utrecht University, 3584 CC Utrecht, The Netherlands. [3]Département de Géographie, Université de Liège, B11-4000 Liège, Belgium. [4]Institute of Geography, University of Bremen, 28359 Bremen, Germany. [5]Institute of Atmospheric and Cryospheric Sciences, University of Innsbruck, A-6020 Innsbruck, Austria.
*e-mail: aimee.slangen@gmail.com

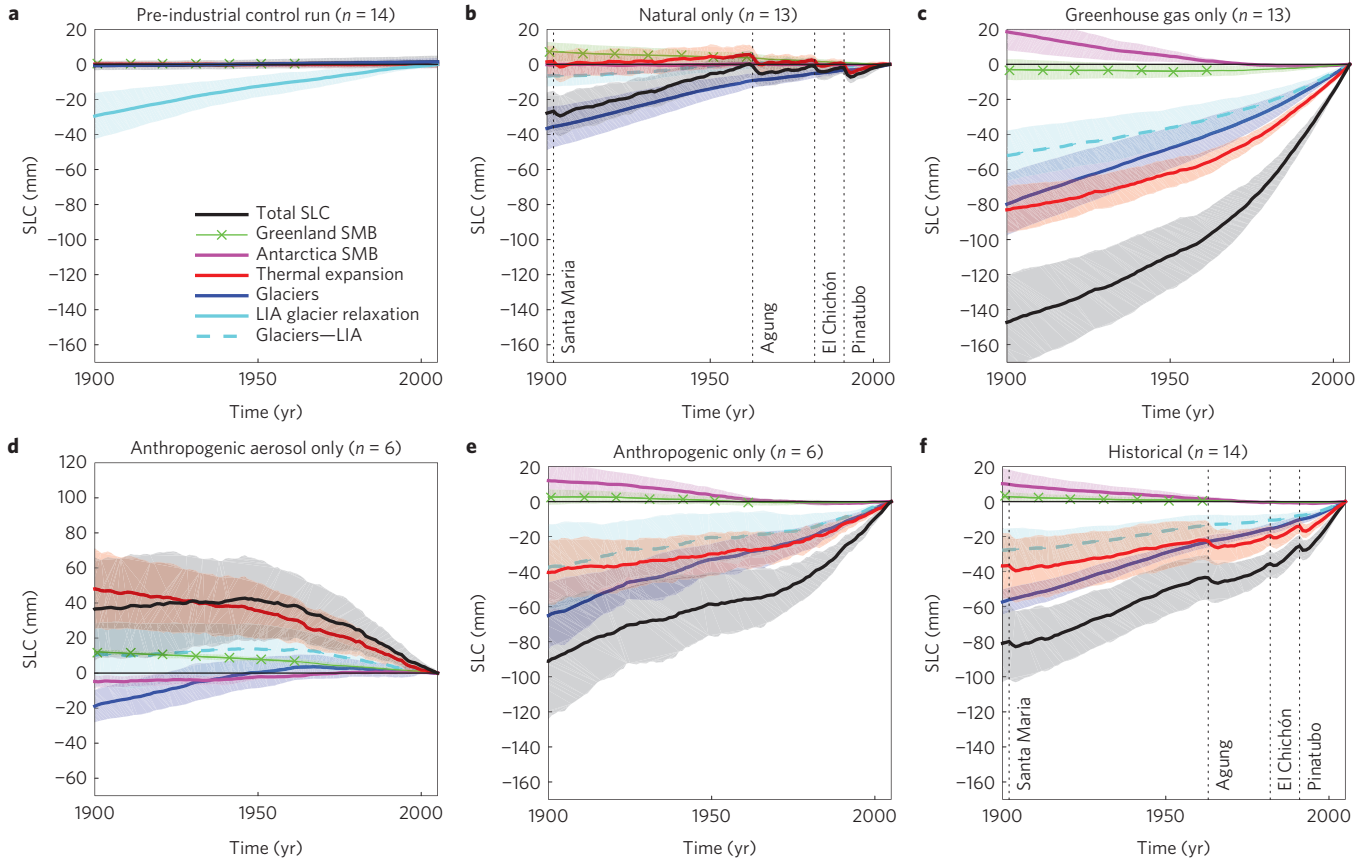

Figure 1 | Cumulative CMIP5 sea-level contributions and the sum for different model experiments, 1900–2005. Results are presented in mm for Greenland SMB, Antarctica SMB, thermal expansion, glaciers and sum with multi-model mean (bold lines) and ±1σ multi-model spread (shaded). **a**, Pre-industrial control runs. **b**, Natural only, indicating major volcanic eruptions (vertical dashed lines). **c**, GHG only. **d**, Anthropogenic aerosol only. **e**, Anthropogenic only. **f**, Historical, including major volcanic eruptions. In **a**, the LIA glacier relaxation contribution is shown in solid cyan; in **b**–**f**, the glacier contribution minus the LIA relaxation is shown in dashed cyan.

Several non-CMIP5 terms are also required to explain the observed GMSLC along with modelled contributions, and thus close the twentieth-century sea-level budget within uncertainties[2,7]. A recent update of the glacier inventory[12] has resulted in more consistent (but smaller) estimates of the twentieth-century glacier contribution than used in previous budget studies[2,7], mainly due to improved glacier hypsometries in the inventory for the Russian Arctic, Svalbard and northern Greenland[13]. With these updates, the glacier contribution driven by CMIP5 data underestimates the change before 1950 when the model is driven by CRU (Climatic Research Unit) gridded data[9], but is not significantly different from observed changes[14] after 1950. The same is found when CMIP5-based Greenland SMB results are compared against reanalysis-driven results (Supplementary Fig. 1). Both differences have been attributed to long-term internal variability in temperatures around Greenland in the reanalysis data that is not present in the CMIP5 model data[15,16], partly because CMIP5 models are not forced to match historical (multi)-decadal variability. We include this difference between reanalysis-driven results and the historical ensemble mean in the twentieth-century sea-level budget (12 mm for glaciers and 15 mm for Greenland SMB; 1900–1950; Supplementary Fig. 1). We also include estimates for groundwater extraction (IPCC AR5 medium estimate: 22 mm; 1900–2005[2,17]), reservoir impoundment (−23 mm; 1900–2005[18]) and observed ice-sheet dynamical processes (4 mm; 1993–2005[19]; assuming no dynamical contribution before 1993). A recent study[20] estimated an observed Greenland ice-sheet contribution of 25 ± 9.4 mm for 1900(LIA)–2010 and ∼22 mm up to 2005, strengthening the basis for our inclusion of a larger Greenland contribution (∼15 mm SMB correction +∼2 mm Greenland dynamics), but acknowledging our estimate may be at the low end of these observations.

The remaining differences between the observations[21–24] (four observation-based reconstructions, see Methods) and CMIP5 models (historical experiment) plus additional terms are approximately linear over the twentieth century (a quadratic fit to the differences reduces the residuals by only 5%, with a variation in the residual trend of only 0.01 mm yr^{-1}). Similar to the glaciers, the ice sheets and the oceans (particularly the deep ocean) may not be in equilibrium at the start of the model simulations in 1850. This non-equilibrium component is solved for here by regressing the residual trends over the period 1970–2005 (when more complete observations are available) against the difference between the modelled and observed TE contribution (Methods, Supplementary Fig. 2). The resulting estimate of 0.13 ± 0.41 mm yr^{-1} is consistent with geologic evidence[25] that constrains a long-term (millennial) sea-level contribution to about 0.2 mm yr^{-1}, with potentially larger contributions from individual ice sheets[7,26].

After adding the non-CMIP5 terms, most of the modelled estimates (except ACCESS 1.3 and GFDL-CM3) agree with the observation ensemble (174 ± 71 mm for 1900–2005) within 2σ uncertainty (Fig. 2, magenta versus black/grey), implying progress in closing the twentieth-century budget, but with the sum of our best estimates still smaller than the observed rise. Five models are found to significantly underestimate the observed TE (from a combination of a smaller GHG and a larger aerosol contribution) for 1970–2005 (Fig. 2, models indicated by light-grey axes in

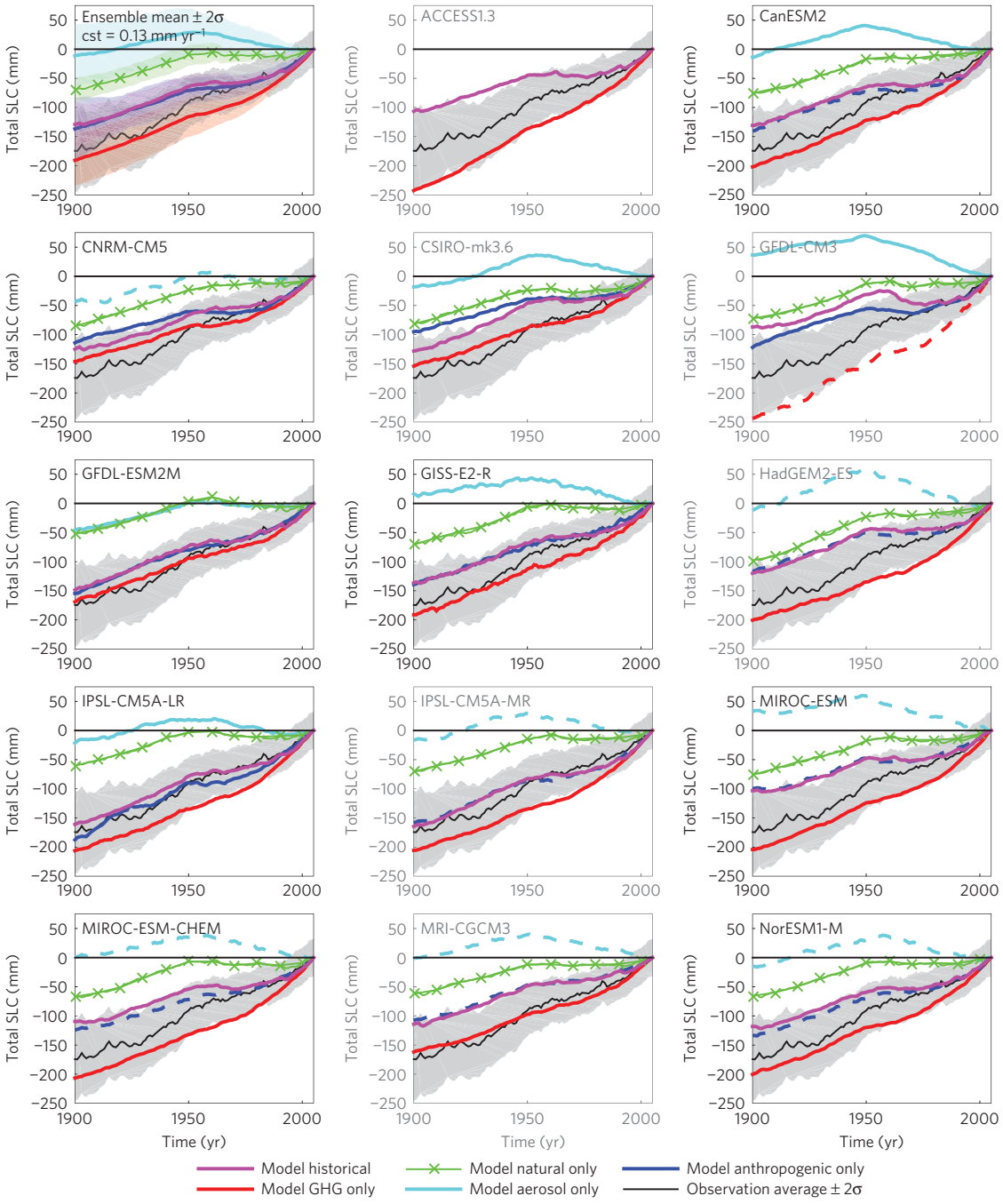

Figure 2 | Comparison of modelled and observational average of cumulative GMSLC time series. Observational average (black line with grey shade $\pm 2\sigma$), model ensemble time series (first panel, $\pm 2\sigma$) and the 14 individual CMIP5 model time series, each showing all available experiments in full lines (includes all CMIP5 + non-CMIP5 contributions, see Supplementary Fig. 3). Missing experiments were derived from the difference between the historical experiment and single-forcing experiments (see Methods) and are plotted in dashed lines. Models with grey axes are outside the 2σ TE range (see Supplementary Fig. 2), and would require the addition of a larger non-equilibrium constant to explain the observed changes.

Fig. 2). A larger non-equilibrium contribution would be required to compensate for this underestimate, and would result in an improved agreement with the observed GMSLC (Supplementary Fig. 2). Excluding these models results in a historical model ensemble mean of 129 ± 39 mm for 1900–2005, compared to 125 ± 44 mm for the full ensemble. Of the four time series used to construct the observation ensemble, three are within the modelled range (ref. 24, the smallest 1900–2005 contribution, 146 ± 51 mm) and only the largest (ref. 23, 200 ± 15 mm) is outside the modelled range.

We add the non-CMIP5 terms to all model experiments (Fig. 2, see Supplementary Fig. 3 for grouping of contributions). For most models, the historical (magenta) and anthropogenic (blue) experiments have a similar magnitude, with more variability in the historical experiment due to the natural forcing. The GHG experiment (red) always has the largest total GMSLC, and for many models exceeds the observed mean GMSLC. In one model (GFDL-ESM2M), the GHG experiment is close to the anthropogenic and historical experiments owing to small aerosol and natural contributions. Before 1950, the aerosol experiments (cyan) are driven mainly by internal climate variability (Glacier and Greenland SMB corrections, non-equilibrium constant and LIA), with a trend similar to the natural-only experiments (green), but without the

Table 1 | Explained fractions (% ± 2σ) for the observation ensemble and each of the four individual reconstructions.

	Historical		Anthropogenic forcing		Natural forcing + internal variability	
	1900–2005	1970–2005	1900–2005	1970–2005	1900–2005	1970–2005
Ensemble	74 ± 22%	87 ± 20%	37 ± 38%	69 ± 31%	38 ± 12%	9 ± 18%
CW11[2]	68 ± 24%	71 ± 19%	39 ± 41%	64 ± 29%	29 ± 13%	1 ± 17%
RD11[3]	81 ± 21%	95 ± 19%	34 ± 35%	67 ± 30%	47 ± 11%	20 ± 18%
J14[4]	68 ± 19%	98 ± 22%	32 ± 33%	76 ± 34%	36 ± 10%	13 ± 20%
HM15[5]	81 ± 27%	85 ± 21%	44 ± 45%	72 ± 32%	38 ± 14%	4 ± 19%

Note that the individual non-equilibrium constants are used (Supplementary Fig. 2) for each of the reconstructions' historical explained fractions.

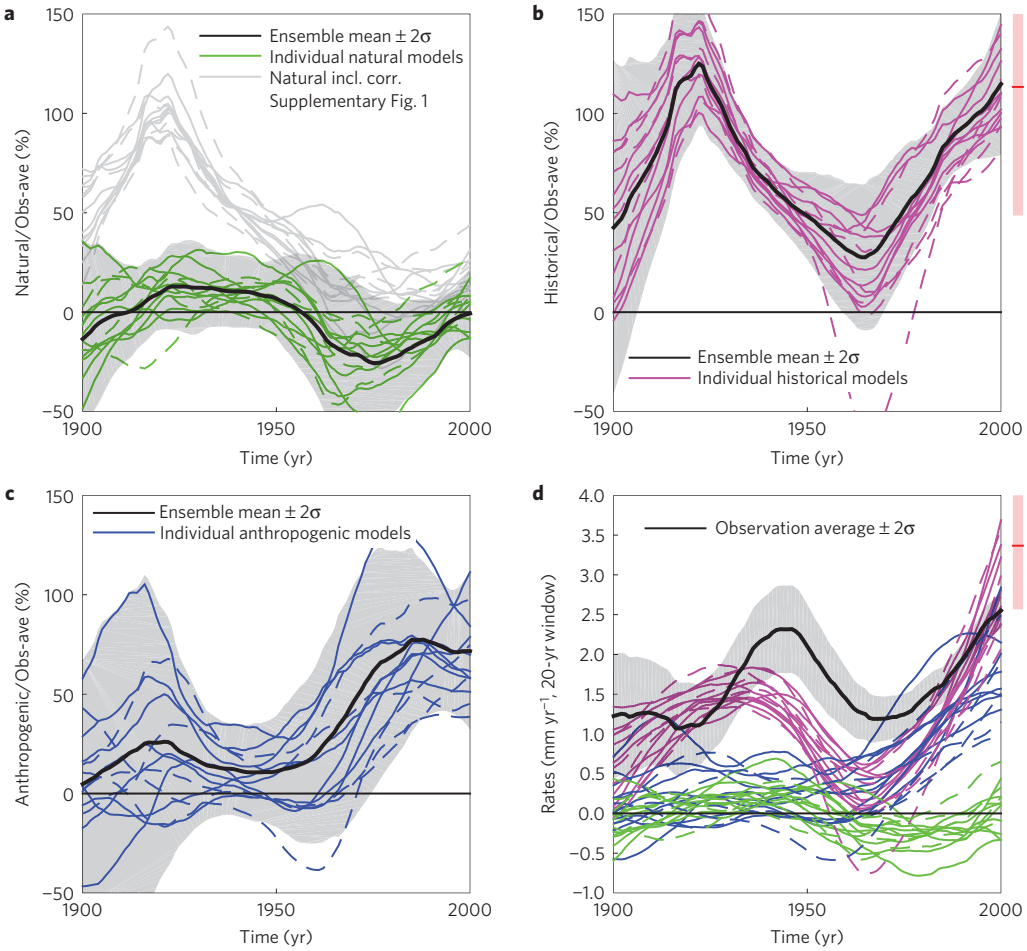

Figure 3 | Explained fractions (%) of total observed sea-level change rates. a, Natural CMIP5 fraction (green) and natural CMIP5 + non-CMIP5 fraction (light-grey lines). **b**, Historical CMIP5 + non-CMIP5 fraction. **c**, Anthropogenic CMIP5 fraction. **d**, Rates used in panels **a** to **c**, with individual models in corresponding colours and the observational average in black line with grey shade (±2σ). Yearly rates are smoothed using a zero-phase filter with a 20-yr window (see Methods; window chosen to improve figure clarity, and does not impact results). Models with dashed lines are outside the 2σ TE range (Supplementary Fig. 2), and not included in the ensemble mean ±2σ (black line with grey shade in **a**–**c**). Red bars outside panels **b** and **d** indicate the 2005–2014 average values, based on IPCC AR5 projections[2] and satellite altimetry observations[27]. Details on included contributions in Supplementary Fig. 3.

natural variability. After 1950, the aerosol experiments have a reduction in GMSLC as a result of the decreased ocean and surface temperatures in response to negative radiative forcing from increased atmospheric aerosol concentrations.

The percentage of the ensemble-mean observed total GMSLC that can be explained by CMIP5 natural forcing alone (without a continuing response to past variations) is 2 ± 15% (1900–2005, from here on all numbers are based on the reduced model ensemble, which excludes models with light-grey axes in Fig. 2, fractions of individual reconstructions in Table 1), and the explained fraction of the observed rate of GMSLC is typically less than 21% (Fig. 3a). If the non-CMIP5 internal variability signals are added to the natural forced experiment (LIA, Glaciers, Greenland SMB and non-equilibrium component), this explains on average 67 ± 23% of the observed change in 1900–1950, but only 9 ± 18% for 1970–2005. When all internal, natural and anthropogenic contributions are included, 74 ± 22% of the total observed change is explained (averaged over the period 1900–2005) and 115 ± 36% of the rate of change in 2000 (Fig. 3b). As a comparison, the 2005–2014 average explained fraction is 113 ± 64%, based on satellite altimetry[27] and IPCC AR5 projections[2] (red bars Fig. 3b/d). This shows that, although the regional pattern as observed by satellite altimetry may

not be captured well by the climate models[28], the global mean change can be accounted for by models fairly well[4].

The CMIP5 anthropogenic component explains 15 ± 55% of the observed change before 1950, and increases to 69 ± 31% for 1970–2005 (Table 1) and 72 ± 39% in 2000 (Fig. 3c). This would increase even further if increased ice-sheet dynamics were considered to be a consequence of increased anthropogenic forcing (to 83% in 2000) and if reservoir storage and groundwater extraction were included (to 94% in 2000). The upper outlier in Fig. 3c, has relatively large rates in the glacier contribution, due to high variability in the Arctic region before 1930.

There are discrepancies between the rates of GMSLC in observations and models (Fig. 3d), most notably from 1940 to 1970, peaking in 1950 (also in individual time series, Supplementary Figs 4–7). This is also reflected in the twentieth-century sea-level budget closure, where models explain 74 ± 22% of the observation ensemble, but a larger percentage for some of the individual reconstructions (Table 1). The differences between models and observations could, for instance, be caused by an internal process in the glaciers or ice sheets, multi-decadal variability in the ocean, or be the result of uncertainties in the reconstructions (because all observational estimates are based on the same limited set of tide gauges, even though the chosen stations and the reconstruction methodologies differ). For each of the four individual observation time series (Supplementary Figs 4–7), the anthropogenic fractions are below 50% up to 1960–1970, increasing to greater than 60% over the last 35 years of the century (Table 1).

Our comprehensive set of simulations demonstrates three main results. First, although natural variations in radiative forcing affect decadal trends, they have little effect over the twentieth century as a whole. Second, in 1900, sea level was not in equilibrium with the twentieth-century climate, and there is a continuing, but diminishing, contribution to sea-level change from this historic variability. Third, the anthropogenic contribution increases during the twentieth century, and becomes the dominant contribution by the end of the century. Our twentieth-century number of 37 ± 38% confirms the anthropogenic lower limit of 45% found in ref. 8. Our results clearly show that the anthropogenic influence is not just present in some of the individual contributors to sea-level change, but actually dominates total sea-level change after 1970.

Methods

Methods and any associated references are available in the online version of the paper.

Received 5 November 2015; accepted 9 March 2016; published online 11 April 2016; corrected online 15 April 2016

References

1. Hinkel, J. *et al*. Coastal flood damage and adaptation costs under 21st century sea-level rise. *Proc. Natl Acad. Sci. USA* **111,** 3292–3297 (2014).
2. Church, J. A. *et al*. in *Climate Change 2013: The Physical Science Basis* (eds Stocker, T. F. *et al*.) 1137–1216 (IPCC, Cambridge Univ. Press, 2013).
3. Marcos, M. & Amores, A. Quantifying anthropogenic and natural contributions to thermosteric sea level rise. *Geophys. Res. Lett.* **41,** 2502–2507 (2014).
4. Slangen, A. B. A., Church, J. A., Zhang, X. & Monselesan, D. Detection and attribution of global mean thermosteric sea-level change. *Geophys. Res. Lett.* **41,** 5951–5959 (2014).
5. Marzeion, B., Cogley, J. G., Richter, K. & Parkes, D. Attribution of global glacier mass loss to anthropogenic and natural causes. *Science* **345,** 919–921 (2014).
6. Taylor, K. E., Stouffer, R. J. & Meehl, G. A. An overview of CMIP5 and the experiment design. *Bull. Am. Meteorol. Soc.* **93,** 485–498 (2012).
7. Gregory, J. M. *et al*. Twentieth-century global-mean sea level rise: is the whole greater than the sum of the parts? *J. Clim.* **26,** 4476–4499 (2013).
8. Dangendorf, S. *et al*. Detecting anthropogenic footprints in sea level rise. *Nature Commun.* **6,** 7849 (2015).
9. Marzeion, B., Jarosch, A. H. & Hofer, M. Past and future sea-level change from the surface mass balance of glaciers. *Cryosphere* **6,** 1295–1322 (2012).
10. Fettweis, X. *et al*. Estimating the Greenland ice sheet surface mass balance contribution to future sea level rise using the regional atmospheric climate model MAR. *Cryosphere* **7,** 469–489 (2013).
11. Roe, G. H. & O'Neal, M. A. The response of glaciers to intrinsic climate variability: observations and models of late-Holocene variations in the Pacific Northwest. *J. Glaciol.* **55,** 839–854 (2009).
12. Arendt, A. A. *et al*. *Randolph Glacier Inventory—A Dataset of Global Glacier Outlines* Version 4.0. (Global Land Ice Measurements from Space, 2014).
13. Marzeion, B., Leclercq, P. W., Cogley, J. G. & Jarosch, A. H. Brief communication: global glacier mass loss reconstructions during the 20th century are consistent. *Cryosphere* **9,** 2399–2404 (2015).
14. Cogley, J. G. Geodetic and direct mass-balance measurements: comparison and joint analysis. *Ann. Glaciol.* **50,** 96–100 (2009).
15. Church, J. A., Monselesan, D., Gregory, J. M. & Marzeion, B. Evaluating the ability of process based models to project sea-level change. *Environ. Res. Lett.* **8,** 014051 (2013).
16. Delworth, T. L. & Zeng, F. Multicentennial variability of the Atlantic Meridional Overturning Circulation and its climatic influence in a 4000 year simulation of the GFDL CM2.1 climate model. *Geophys. Res. Lett.* **39,** L13702 (2012).
17. Wada, Y. *et al*. Past and future contribution of global groundwater depletion to sea-level rise. *Geophys. Res. Lett.* **39,** L09402 (2012).
18. Chao, B. F., Wu, Y. H. & Li, Y. S. Impact of artificial reservoir water impoundment on global sea level. *Science* **320,** 212–214 (2008).
19. Shepherd, A. *et al*. A reconciled estimate of ice-sheet mass balance. *Science* **338,** 1183–1189 (2012).
20. Kjeldsen, K. K. *et al*. Spatial and temporal distribution of mass loss from the Greenland Ice Sheet since AD 1900. *Nature* **528,** 396–400 (2015).
21. Church, J. A. & White, N. J. Sea-level rise from the late 19th to the early 21st century. *Surv. Geophys.* **32,** 585–602 (2011).
22. Ray, R. D. & Douglas, B. C. Experiments in reconstructing twentieth-century sea levels. *Prog. Oceanogr.* **91,** 496–515 (2011).
23. Jevrejeva, S., Moore, J. C., Grinsted, A., Matthews, A. P. & Spada, G. Trends and acceleration in global and regional sea levels since 1807. *Glob. Planet. Change* **113,** 11–22 (2014).
24. Hay, C. C., Morrow, E., Kopp, R. E. & Mitrovica, J. X. Probabilistic reanalysis of twentieth-century sea-level rise. *Nature* **517,** 481–484 (2015).
25. Masson-Delmotte, V. M. *et al*. in *Climate Change 2013: The Physical Science Basis* (eds Stocker, T. F. *et al*.) 383–464 (IPCC, Cambridge Univ. Press, 2013).
26. Church, J. A. *et al*. Revisiting the Earth's sea-level and energy budgets from 1961 to 2008. *Geophys. Res. Lett.* **38,** L18601 (2011).
27. Watson, C. S. *et al*. Unabated global mean sea-level rise over the satellite altimeter era. *Nature Clim. Change* **5,** 565–568 (2015).
28. Bilbao, R. A. F., Gregory, J. M. & Bouttes, N. Analysis of the regional pattern of sea level change due to ocean dynamics and density change for 1993–2099 in observations and CMIP5 AOGCM's. *Clim. Dynam.* **45,** 2647–2666 (2015).

Acknowledgements

We acknowledge the World Climate Research Programme's Working Group on Coupled Modelling, which is responsible for CMIP, and we thank the climate modelling groups (listed in Supplementary Table 1) for producing and making available their model output. For CMIP, the US Department of Energy's Program for Climate Model Diagnosis and Intercomparison provides coordinating support and leads development of software infrastructure in partnership with the Global Organization for Earth System Science Portals. A.B.A.S. is supported by a CSIRO Office of the Chief Executive Fellowship and the NWO-Netherlands Polar Program. J.A.C. is partially supported by the Australian Climate Change Science Program. B.M. and K.R. were supported by the Austrian Science Fund (FWF): P25362-N26, and by the Austrian Ministry of Science BMWF as part of the UniInfrastrukturprogramm of the Focal Point Scientific Computing at the University of Innsbruck.

Author contributions

J.A.C. and B.M. initiated the study. A.B.A.S. provided the thermal expansion data, carried out the analysis together with J.A.C. and produced the figures. B.M. and K.R. provided the glacier model data. X.F. and C.A. provided the ice sheet SMB model data. A.B.A.S. led the writing with the assistance of J.A.C., and all authors contributed to the writing of the manuscript.

Additional information

Supplementary information is available in the online version of the paper. Reprints and permissions information is available online at www.nature.com/reprints. Correspondence and requests for materials should be addressed to A.B.A.S.

Competing financial interests

The authors declare no competing financial interests.

Methods

Models. Output from five experiments in the CMIP5 climate model database[6] are used to estimate sea-level contributions under different external forcings: historical (all-forcing, 14 models), anthropogenic-only (6 models), natural-only (13 models), GHG-only (13 models) and anthropogenic aerosol-only (6 models), for 1850–2005 (Supplementary Table 1). The model selection is based on the availability of all required variables and the presence of at least one experiment in addition to the historical-all-forcing experiment. Only the first available realization is used. Pre-industrial control runs (14 models) are used to estimate internal climate variability.

As not all models provided all five external-forcing experiments, the missing experiments were derived from the difference between historical runs and single-forcing runs, while accounting for the glacier LIA contribution. Linearity is assumed in the response to the external forcings[4] (dashed lines in Fig. 2), using the following relations in the remainder of the study: Anthropogenic = Historical–Natural (7 models); GHG = Historical–(Natural + Aerosol) (1 model); and Aerosol = Historical–(Natural + GHG) (7 models). The ACCESS 1.3 model provided only a historical and a GHG experiment, which is not enough to derive the missing experiments. The influence of the addition of the derived runs on the multi-model ensemble mean is small, amounting to +5.1 mm for the Aerosol ensemble, +4.1 mm for the GHG ensemble and +3.3 mm for the Anthropogenic ensemble over the period 1900–2005.

The thermal expansion (TE) contribution is taken directly from the CMIP5 model database (variable name zostoga) and is corrected for model drift using the pre-industrial control runs[29].

The glacier contribution is obtained by driving a global glacier evolution model[9] with temperature and precipitation from the CMIP5 models determining the mass balance change of individual glaciers in the Randolph Glacier Inventory v4.0 (ref. 12). If the glacier model is spun up for 500 years under control run forcing and then driven by pre-industrial control conditions for another 500 years, the glacier contribution over the latter 500 years is small (dark blue, Fig. 1a).

For the Greenland ice-sheet surface mass balance (SMB) contribution, the regional climate model MARv3.5[10] is forced with a limited number of CMIP5 models (MIROC5-historical over the period 1900–2005, NorESM1-historical over the period 1950–2005 and CanESM1-historical over the period 1950–2005), given the large computational requirements of MAR. The output from these simulations is used to establish a statistical relationship between CMIP5 annual snowfall over Greenland, atmospheric summer temperature at 600 hPa and the Greenland surface mass balance[10], resulting in:

$$\mathrm{SMB_{MAR}} = \mathrm{SF_{CMIP5}} \times 2 - \mathrm{TT_{CMIP5}} \times 50 \quad (1)$$

where TT = average June–July–August air temperature (CMIP5 variable TA) at 600 hPa (20–70° W; 60–85° N) and SF = annual snowfall in mm $\mathrm{yr^{-1}}$ (CMIP5 variable PRSN, 20–70° W; 65–80° N).

The Antarctic ice-sheet SMB contribution is estimated by taking the CMIP5 precipitation minus evaporation over the Antarctic ice sheet. Although snow-pack processes over the ice sheets are usually not correctly modelled in CMIP5 models, runoff is negligible for present climate[30], and evaporation accounts for less than 10% of the P–E changes. To account for the fact that the percentage change in SMB varies linearly with temperature, the time series are rescaled so that their mean for 1985–2005 fits the best estimate of total grounded ice-sheet SMB (~1980 Gt $\mathrm{yr^{-1}}$ for 1979–2010, from the regional climate model RACMO2 forced by ERA-Interim[30]).

Observations. The modelled total GMSLC of the historical CMIP5 experiments is compared against (the average of) four different global mean sea-level reconstructions: Ray and Douglas[22], Jevrejeva *et al.*[23], Church and White[21] and Hay *et al.*[24]. Each of these reconstructions is based on tide-gauge observations, but differ in the way the temporal and spatial distribution of the data is dealt with. The most recent version of each reconstruction is selected, and the period 1900–2005 is used: 1900 because all four reconstructions have data and 2005 because that is the final year for most historical CMIP5 model experiments. The average of the four observational estimates of total sea-level change is 174 ± 71 mm over the period 1900–2005. Ref. 24 has the smallest 1900–2005 cumulative contribution (146 ± 25 mm), and ref. 23 the largest (200 ± 8 mm). Leaving out any one of them would at most lead to differences of ± 9 mm in the observational average.

Derivation of the non-equilibrium constant. Supplementary Fig. 2 shows that the constant value required to optimally close the 1970–2005 budget differs for each model, and is linearly related to the difference between TE models and observations for that same period. This suggests that (part of) the mismatch between observations and models is due to the limited ability of the models to simulate (deep) ocean TE changes. Instead of using the model-dependent and highly varying values as non-equilibrium (ice sheet/deep ocean TE) constants, we use this linear relation to find the one optimized trend value where the 1970–2005 difference between TE observations and models is zero (Supplementary Fig. 2). The choice for 1970–2005 instead of 1900–2005 as reference period is based on the better quality of observations for 1970–2005. An optimal fit for 1900–2005 would result in a better closure of the cumulative twentieth-century sea-level budget, but would also reduce the 1970–2005 budget closure (the modelled GMSLC would be too large), which is undesirable given the better data quality in the more recent period.

Explained fractions. Explained fractions are computed as the modelled sea-level change divided by the observed sea-level change. All fractions presented in the main text are based on the reduced model ensemble—that is, excluding the models with light-grey axes in Fig. 2. The reason for the exclusion is that they are outliers in the analysis in Supplementary Fig. 2. The impact of the reduced ensemble is maximum 5%, depending on the experiment. Explained fractions for periods (for example, the twentieth century) are computed using the cumulative sea-level change, as shown in Fig. 2. Explained fractions for specific years (for example, 1900, 2000) are computed using the yearly rates of change in a zero-phase digital filter with a window of 20 years (Matlab function: *filtfilt*(*ones*(*1,20*)/*20,1,yearly_rates*)). This function filters data in forward and reverse directions, has no phase distortion and minimizes end effects by matching initial conditions, allowing one to specify a value in 2000.

References

29. Sen Gupta, A., Jourdain, N. C., Brown, J. N. & Monselesan, D. Climate drift in CMIP5 Models. *J. Clim.* **26,** 8597–8615 (2013).
30. Lenaerts, J. T. M., van den Broeke, M. R., van de Berg, W. J., van Meijgaard, E. & Munneke, P. K. K. A new, high-resolution surface mass balance map of Antarctica (1979–2010) based on regional atmospheric climate modeling. *Geophys. Res. Lett.* **39,** L04501 (2012).

Erratum: Anthropogenic forcing dominates global mean sea-level rise since 1970

Aimée B. A. Slangen, John A. Church, Cecile Agosta, Xavier Fettweis, Ben Marzeion & Kristin Richter

Nature Climate Change http://dx/doi/org/10.1038/nclimate2991 (2016); published online 11 April 2016; corrected online 15 April 2016

In the version of this Letter originally published, in the paragraph above equation 1 in the Methods section, a percentage value was mistakenly included due to a typographical error. This error has been corrected in all versions of the Letter.